CME-FLARE ASSOCIATION DEDUCED FROM CATASTROPHIC MODEL OF CMES

JUN LIN
Harvard-Smithsonian Center for Astrophysics, 60 Garden Street, Cambridge, MA 02138, U.S.A.

(Received 10 April 2003; accepted 13 October 2003)

Abstract. Based on our previous works regarding solar eruptions, we focus on the relationships among different eruptive phenomena, such as solar flares, eruptive prominences and coronal mass ejections (CMEs). The three processes show clear correlations under certain circumstances. The correlation between a CME and solar flare depends the energy that stored in the relevant magnetic structure, which is available to drive the eruption: the more energy that is stored, the better the correlation is; otherwise, the correlation is poor. The correlation between a CME and eruptive prominence, on the other hand, depends on the plasma mass concentration in the configuration prior to the eruption: if the mass concentration is significant, a CME starts with an eruptive prominence, otherwise, a CME develops an without an apparent associated eruptive prominence. These results confirm that solar flares, eruptive prominences and CMEs are different significances of a single physical process that is related to the energy release in a disrupted coronal magnetic field. The impact of gravity on CME propagation and the above correlations is also investigated. Our calculations indicate that the effect of gravity is not significant unless the strength of the background field in the disrupted magnetic configuration becomes weak, say weaker than 30 G.

1. Introduction

The correlation between solar flares and coronal mass ejections (CMEs) was first discussed by Gosling *et al*. (1976) based on *Skylab* observations, and then by MacQueen and Fisher (1983) and Harrison (1986) based on the K-coronameter, more recently by Dere *et al*. (1999), Neupert *et al*. (2001), and Zhang *et al*. (2001) based on LASCO observations, and by Alexander, Metcalf, and Nitta (2002) based on both LASCO and *Yohkoh* observations. Zhang *et al*. (2001) showed that the early impulsive acceleration phase of CMEs coincides very well with the rise of the associated X-ray flares, and the increase in the CME speed always corresponds to the increase of the soft X-ray flux. Related to this correlation is the classification of CMEs, and the mechanisms for various observed CMEs. Speed is usually a criterion used to distinguish two types of CMEs: slow (gradual) CMEs and fast (impulsive) CMEs. Slow CMEs normally show gentle and continuous propagations with speed less than 500 km s^{-1} and the maximum of acceleration less than 100 m s^{-2} (Srivastava *et al*., 1999); while fast CMEs usually manifest energetic behaviour with speed larger than 500 km s^{-1} and the maximum of acceleration larger than 100 m s^{-2}, those with speed larger than 2000 km s^{-1} and the maximum of acceleration larger than 1000 m s^{-2} are also reported sometimes (Zhang *et al*.,

Solar Physics **219:** 169–196, 2004.

2001). Although they did not deal with acceleration, Gosling *et al*. (1976) already noticed that flare-associated CMEs traveled faster (~ 800 km s^{-1}) than events associated with eruptive prominences (330 km s^{-1}), and an event without an associated flare was generally slower than 360 km s^{-1}.

Based on analyzing the data from LASCO alone, Andrews and Howard (2001) suggest that CMEs be classified into type A, which show acceleration in the field of view of LASCO/C2, and type C, which show constant velocity in the same field of view. This classification is not new. MacQueen and Fisher (1983) analyzed 12 well observed coronal transients, namely CMEs. They concluded that those events represented two classes that could be clearly delineated based on plots of radial velocities versus height. They identified the two classes as flare-associated impulsive events with a constant speed, and eruptive prominence-associated events that show significant acceleration. They believe that the two classes of eruptions may be fundamentally different. However, we must keep in mind that the occulting disk of coronagraphs commonly blocks part of the corona at lower attitude, and the initial stage of an eruption usually cannot be well observed by coronagraphs. As the observations near the solar surface become available, both fast and slow CMEs manifest apparent acceleration at initial stage (Srivastava *et al*., 1999; Alexander, Metcalf, and Nitta, 2002; Burkepile, Darnell, and DeToma, 2002; Wang *et al.* 2003).

As many authors tried to find and discuss differences between CMEs associated with flares and those without flares (e.g., Gosling *et al*., 1976; MacQueen and Fisher, 1983; Kahler, 1992; Dryer, 1996; Sheeley *et al*., 1999; Andrews and Howard, 2001), Švestka (1986) instead pointed out at the first place that in both cases the cause of the CME is the same, the only difference between flare-associated and non-flare-associated CMEs is the strength of the magnetic field in the region where the eruption is initiated (see also Švestka and Cliver, 1992; Švestka, 1995), and that the correlations between solar flare and CME vary continuously with the strength of the relevant magnetic field (Z. Švestka, 2002, private communication) and no sharp boundary exists separating good and poor correlations. This statement can be verified via both observations and theoretical calculations.

For the first time, Zhang *et al*. (2002) quantitatively investigated the correlations of CMEs with solar flares via studying variations of the time of flare at maximum versus the speed of the associated CME. By analyzing the flare data from TRACE, the CME data from LASCO, as well as the GOES X-ray flux data that were used to determine the maxima of flares, they found that the faster the CME is, the earlier the associated flare reaches the maximum, and that the association of fast CMEs with flares is better and more apparent than that of slow CMEs with flares. Among the samples they chose, most X-class flares (12 out of 13) went with fast CMEs, more than half (18 out of 30) fast CMEs in turn are associated with M-class flares, and only one X-class flare was associated with a slow CME. In a similar study conducted by Moon *et al*. (2002), the fraction of CMEs associated with flares

among the total of 3217 CMEs analyzed has a tendency to increase with the CME speed.

The results of Moon *et al*. (2002) show that less than 5% of slow (≤ 200 km s^{-1}) CMEs were associated with flares, and the fraction approaches 15% as CME speed reaches 1000 km s^{-1}. But the values of these fractions can only be considered as a lower limit since Moon *et al*. (2002) set up an overly strict confinement of their samples such that those CMEs associated with both flares and eruptive prominences were ruled out. However, their conclusion still replicates that of Zhang *et al*. (2002) in an alternative way. For the eruptions occurring during the solar minimum, the above correlation still holds: slow CMEs are poorly associated with other activities on the surface, the average speed of the CMEs with rigorously associated activity is obviously higher than that of the unassociated CMEs (Wagner, 1984; St. Cyr and Webb, 1991).

Low and Zhang (2002) discussed the above CME–flare association based on their qualitative theory, and conclude that observation is consistent with their theory. But it is not quite clear whether any definite and quantitative conclusion could be drawn from their work since they did not provide any quantitative specification of how the magnetic configurations in their model would eventually evolve as the eruption occurs, how the CME velocities would be calculated from their model, and how the times of flare at maxima could be deduced according to their qualitative theory. Meanwhile, Lin (2002) also intended to understand the physics that may be revealed by the above correlations. Based on the results calculated from the catastrophic models of CMEs, Lin pointed out that the property of the correlations of CMEs to solar flares is governed by the free energy (namely the difference between the non-potential energy and the corresponding potential energy) stored in the relevant magnetic configuration prior to the eruption.

The conclusion of Lin (2002) was drawn according to the qualitative discussions about the main results deduced from the calculations based on the work of Lin and Forbes (2000). For simplicity of mathematics, Lin and Forbes (2000) totally ignored gravity when constructing an analytical model of CMEs during its dynamic process. Low (2001) noted that gravity plays an important role in the CME process, especially at the initial stage of eruption.

To look into the CME–flare association in more detail, in the next section we are going to modify a specific catastrophic model for CMEs (see Forbes and Priest, 1995; Lin and Forbes, 2000; Lin, 2002) by including gravity. In Section 3, we shall investigate the output powers during eruptive processes and the corresponding CME velocities, discuss the observational consequences of the relevant results, and then compare them with the observational results of Zhang *et al*. (2002). In Section 4, we will investigate the dependence of energetics of an eruptive process on the strength of the magnetic field involved and discuss the implications of this relationship to both the classifications of CMEs and the correlations between CMEs and flares. In Section 5, we compare the correlation between CMEs and solar flares with that between CMEs and eruptive prominences, and briefly discuss

the difference in physics between the two correlations. Finally, we summarize the present work in Section 6.

2. Synopsis of Previous Works and Important Formulae

In case the readers are not aware of our previous works, we here briefly outline the relevant results and important conclusions deduced under the framework of the catastrophic models of CMEs developed by Forbes and Isenberg (1991) based on the similar ideas originally raised by Van Tend and Kuperus (1978) and Van Tend (1979). The catastrophic loss of equilibrium occurring in a coronal magnetic configuration somehow re-activates the Kopp–Pneuman-type models of solar eruptions (see Kopp and Pneuman (1976)). The closed magnetic field in the corona is so stretched in the catastrophic process that it is usually thought 'open' to infinity and a local Kopp–Pneuman structure forms including a thin current sheet (Figure 1). Magnetic reconnection invoked by plasma instabilities inside the current sheet eventually not only creates the separating flare ribbons on the solar disk and growing post-flare loop systems in the corona (see the enlargement at the bottom of Figure 1 and also refer to a recent review by Forbes, 2003), but also helps the extended part of the magnetic structure escape into the outermost corona and interplanetary space (see also Lin and Forbes, 2000; Forbes and Lin, 2000; and Lin, 2002, for more discussions), resulting in CMEs and the consequent disturbance in space. Furthermore, the non-ideal MHD properties of magnetic reconnection lead to the problem of opening the closed magnetic field by a purely MHD process, also known as the Aly–Sturrock paradox (Aly, 1991; Sturrock, 1991), which was first raised by Aly (1984), to being thus avoided (refer to Lin, 2001, for more details). Figure 1 schematically indicates how a CME process in the high corona and space (see also Lin and Forbes, 2000) is intrinsically related to a traditional two-ribbon flare process (see Forbes and Acton, 1996, and the references therein; and Švestka and Cliver, 1992, and the references therein).

To introduce a proper mathematical description of the above process, we use Figure 2 to sketch a diagram of the disrupted magnetic configuration that includes a current-carrying flux rope which is usually used to model the prominence or the filament, and to show the mathematical notations that will be used in the text. The photosphere (or, more properly, the base of the corona) is located at $y = 0$ in the $x - y$ plane, the center of the flux rope is located at $(0, h)$ and the two-point source regions each with flux $\pi I_0/c$ on the photosphere are separated by a distance of 2λ. At time t, a force-free flux rope with radius r_0 is located at height h on the y-axis. Below it there may exist a detached vertical current sheet along the y-axis with its lower tip at $y = p$ and upper tip at $y = q$. Generally, a magnetic configuration like this is not necessarily in equilibrium, especially as the magnetic reconnection occurs in the current sheet. The characteristic values of the above important parameters and the basic equations governing the dynamic properties of

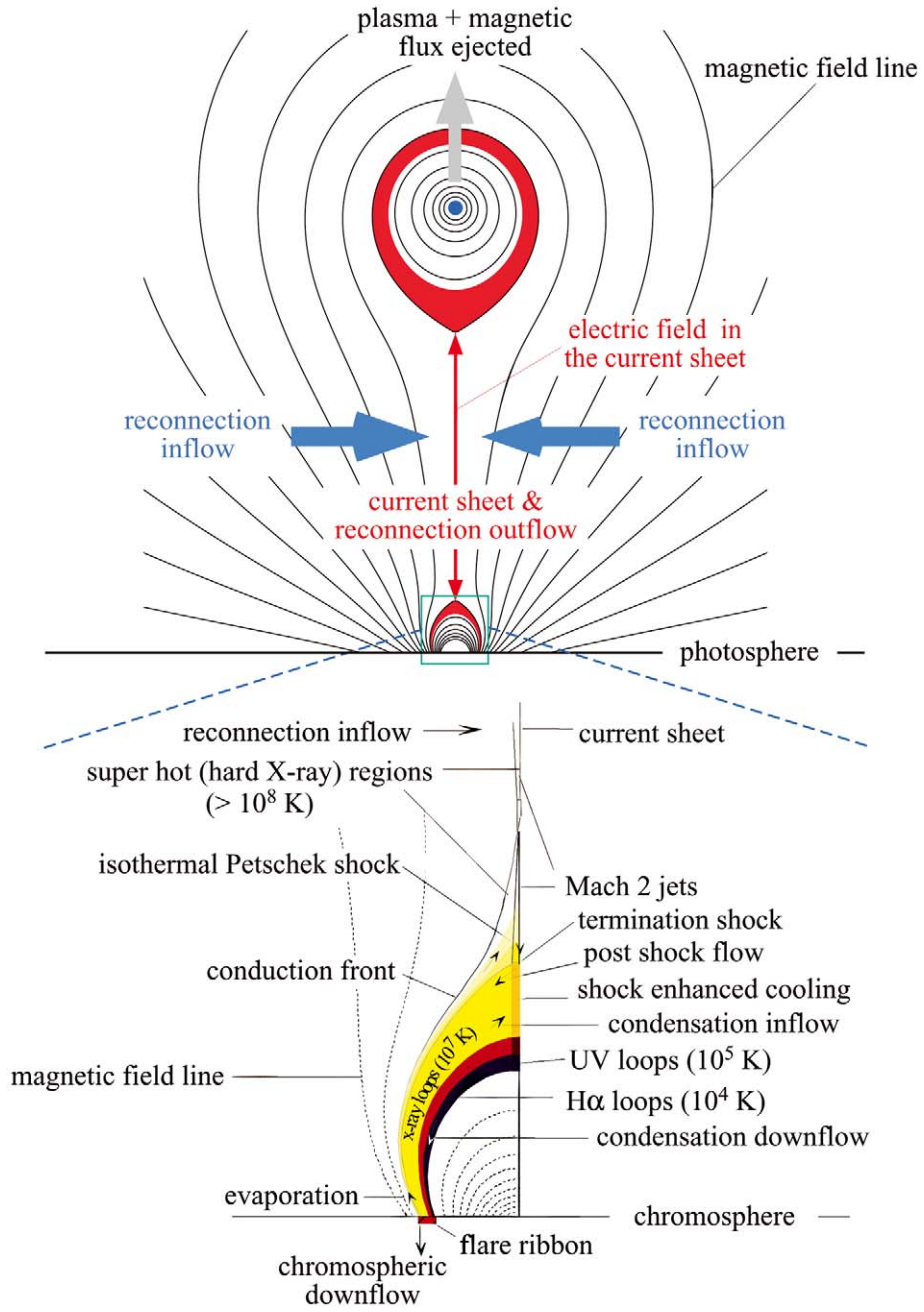

Figure 1. Schematic diagram of a disrupted magnetic field that forms in an eruptive process. Catastrophic loss of equilibrium, occurring in a magnetic configuration including a flux rope, stretches the closed magnetic field and creates a Kopp–Pneuman-type structure. This diagram is created by incorporating the traditional two-ribbon flare model (*bottom*, from Forbes and Acton, 1996) with the CME model (*top*) of Lin and Forbes (2000). Colors denote the different hierarchies of plasma in the configuration.

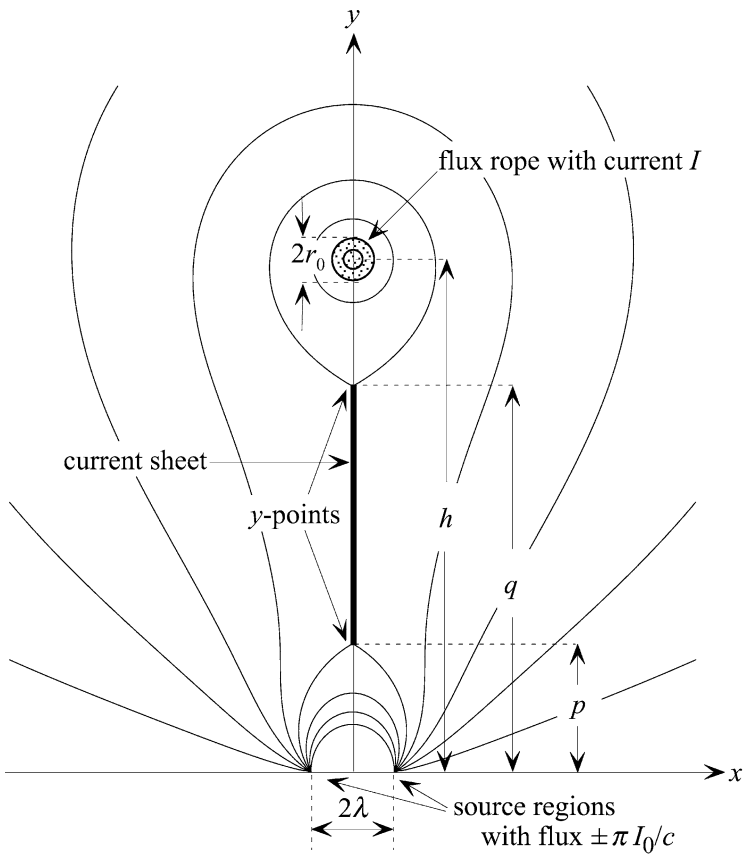

Figure 2. Diagram of the relevant magnetic configuration showing the mathematical notations used in the text. (From Lin and Forbes, 2000.)

the system used by Lin and Forbes (2000) can still be used in the present work. For illustrative purposes, we list those characteristic values here:

$$\lambda_0 = 5 \times 10^4 \text{ km}, \qquad m = 2.1 \times 10^6 \text{ g cm}^{-1},$$
$$r_{00} = 0.1\lambda_0, \qquad \rho_0 = 1.673 \times 10^{-14} \text{ g cm}^{-3},$$
$$I_0/c\lambda_0 = 50 \text{ G}, \qquad \dot{h}_0 = 1000 \text{ km s}^{-1},$$

where λ_0 is the length scale, m is the mass per unit length inside the flux rope, r_{00} is the initial value of the flux rope radius, ρ_0 is the mass density at the base of the corona, $2I_0\sigma/c\lambda_0$ is the background field strength at the origin (refer to Figure 2), I_0 is a constant with dimensions of electric current and is also the scale of the electric current inside the flux rope, c is the light speed, σ is a dimensionless constant which is used to adjust the strength of the background field, and $\dot{h}_0$ is the scale of velocity, which will be used to normalize the flux rope velocity $\dot{h}$. The extension of the flux rope (prominence) in the z-direction is typically of order of

10^5 km (Priest, 1982), so that the total mass contained in the flux rope is about 2.1×10^{16} g. In reality, a CME typically sends as much as 10^{15}–10^{16} g of plasma into the outermost corona and interplanetary space (Hundhausen, 1988).

As demonstrated by Forbes and Priest (1995), the gradual evolution of the system in response to the slow converging motion of the source regions on the photosphere eventually results in a catastrophic loss of mechanical equilibrium in the system, leading the magnetic compression to thrusting the flux rope upward. In this specific configuration (refer to Figure 2 of Forbes and Priest, 1995), only after the onset of the eruption does a reconnection site, such as a neutral point or a current sheet, form. So, the eruptions taking place in this kind of magnetic structure will always manifest heating, and thus flares, following the take-off of the associated CMEs. We are discussing the configurations that give rise to flares first shortly.

The consequent dynamical evolution of the system following the formation of the current sheet is governed by a set of ordinary differential equations that were deduced by Lin and Forbes (2000):

$$\begin{aligned} \frac{\mathrm{d}p}{\mathrm{d}t} &= \frac{6}{5}p'\dot{h}, \qquad \frac{\mathrm{d}q}{\mathrm{d}t} = \frac{6}{5}q'\dot{h}, \\ \frac{\mathrm{d}\dot{h}}{\mathrm{d}t} &= \frac{6}{5}\dot{h}'\dot{h}, \qquad \frac{\mathrm{d}h}{\mathrm{d}t} = \frac{6}{5}\dot{h}, \end{aligned} \tag{1}$$

where p and q denote the heights of the lower and the higher tips of the current sheet, respectively, the prime ($'$) means taking a derivative with respect to h, and the time t is in units of minutes. The factor of 6/5 exists from the normalizations of the units. The expressions for p', q', and $\dot{h}'$ are listed in Equation (43) of Lin and Forbes (2000). In order to save space, we do not duplicate them all here, but we need to point out that Lin and Forbes (2000) did not consider gravity in their calculations and only the case corresponding to $\sigma = 1$ was investigated. Therefore, some essential modifications for the expressions for p', q', and $\dot{h}'$ are necessary.

First, Equation (36) of Lin and Forbes (2000) now becomes

$$m\dot{h}\dot{h} = \left(\frac{I_0}{c}\right)^2 \frac{\lambda^2\sigma^2}{2hL_{PQ}^2}\left[\frac{H_{PQ}^2}{2h^2} - \frac{(\lambda^2+p^2)(h^2-q^2)}{\lambda^2+h^2} - \right.$$
$$\left. - \frac{(\lambda^2+q^2)(h^2-p^2)}{\lambda^2+h^2}\right] - \frac{mg_\odot}{(1+h/R_\odot)^2},$$

where $g_\odot = 2.74 \times 10^4$ cm s^{-2} and $R_\odot = 6.96 \times 10^{10}$ cm are the surface gravity and the radius of the Sun, respectively, $L_{PQ}^2 = (\lambda^2+p^2)(\lambda^2+q^2)$, and $H_{PQ}^2 = (h^2-p^2)(h^2-q^2)$. Normalizing this equation according to the characteristic values of the parameters given above yields:

$$\dot{h}\dot{h}' = \frac{2.5\lambda^2\sigma^2}{1.68hL_{PQ}}\left[\frac{H_{PQ}^2}{2h^2} - \frac{(\lambda^2+p^2)(h^2-q^2)}{\lambda^2+h^2} - \right.$$
$$\left. - \frac{(\lambda^2+q^2)(h^2-p^2)}{\lambda^2+h^2}\right] - \frac{1.37\times10^{-2}}{(1+5h/69.6)^2}, \tag{2}$$

which suggests that the impact of gravity could be trivial unless the eruption occurs in a configuration with a fairly weak background field (small σ).

Second, the parameter $\tilde{A}_{0h}$, which relates the evolutionary behaviors of the system to the rate of magnetic reconnection occurring in the current sheet (see Equation (43) of Lin and Forbes (2000)) reads as[1]

$$\tilde{A}_{0h} = \frac{c}{2I_0}\frac{M_{\rm A}B_y^2(0,y_0)}{\sigma\dot{h}\sqrt{4\pi\rho(y_0)}} + A_{0h}, \tag{3}$$

where $M_{\rm A}$, the Alfvén Mach number of magnetic reconnection, is the speed of reconnection inflow towards the current sheet in units of the local Alfvén speed, the parameter A_{0h} is the same as that given in Equation (28) of Lin and Forbes (2000) and no modification for it is needed in the present work, $\rho(y) = \rho_0 f(y)$ depicts the variation of the plasma density versus the altitude y in the corona and $f(y)$ is a dimensionless function of y with $f(0) = 1$, ρ_0 is the value of $\rho(y)$ at $y = 0$, which is taken as 1.673×10^{-14} g cm^{-3} in the present work, $y_0 = (p+q)/2$ is the height of the mid-point of the current sheet, and $B_y(0, y_0)$ is the y component of magnetic field at the mid-point of the current sheet $(0, y_0)$. The dependences of $B_y(0, y)$ and $f(y)$ on the altitude y are given by (see Lin and Forbes, 2000; Lin, 2002; and Sittler and Guhathakurta, 1999)

$$B_y(0,y) = \frac{2I_0}{c\lambda_0}\frac{\sigma\lambda(h^2+\lambda^2)}{(h^2-y^2)(y^2+\lambda^2)}\sqrt{\frac{(y^2-p^2)(q^2-y^2)}{(\lambda^2+p^2)(\lambda^2+q^2)}} \tag{4}$$

and

$$f(y) = a_1 z^2(y) e^{a_2 z(y)}\left[1 + a_3 z(y) + a_4 z^2(y) + a_5 z^3(y)\right], \tag{5}$$

respectively, where

$$z(y) = 1/(1+5y/69.6), \qquad a_1 = 0.001272,$$
$$a_2 = 4.8039, \qquad a_3 = 0.29696,$$
$$a_4 = -7.1743, \qquad a_5 = 12.321.$$

Here, the empirical model of the coronal plasma density shown in Equation (5) was developed by Sittler and Guhathakurta (1999) on the basis of those constructed from *Skylab* white-light coronagraph observations (Guhathakurta, Holzer, and MacQueen, 1996) and *in situ* plasma measurement by *Ulysses* (Phillips *et al.*,

[1]The factor $c/2I_0$ in the same equation given by Lin and Forbes (2000) was missed.

1995). It decreases exponentially for small y as the plasma density does in the lower corona (isothermal atmosphere), and then decreases with height quadratically in the outermost corona and interplanetary space. The two functional behaviors are smoothly connected at the altitude of $\sim 0.7\ R_\odot$ (see Figure 1 of Lin, 2002). The results of radio observations of type III bursts over a wide waveband from a few kHz to 13.8 MHz also suggest a $1/y^2$ variation of the plasma density far from the Sun (Leblanc, Dulk, and Bougeret 1998). Substituting Equations (4), (5) and expression for $\rho(y)$ into (3), and making the necessary normalizations, we have

$$\tilde{A}_{0h} = \frac{2.18 M_{\rm A}\sigma}{\dot{h}\sqrt{f(y_0)}} \left[\frac{\lambda(h^2+\lambda^2)}{(h^2-y_0^2)(y_0^2+\lambda^2)}\right]^2 \frac{(y_0^2-p^2)(q^2-y_0^2)}{(\lambda^2+p^2)(\lambda^2+q^2)} + A_{0h}. \tag{6}$$

The third modification we have to make is for the stage of the evolution in the system from the loss of equilibrium to the formation of the current sheet. Forbes and Priest (1995) and Lin and Forbes (2000) have investigated the evolution at this stage for the case of $\sigma = 1$ and neglecting gravity. Including gravity and considering the variations in the strength of the background field, we obtain the force acting on the flux rope per unit length prior to the formation of the current sheet:

$$F = \left(\frac{I_0}{c}\right)^2 J\left[\frac{J}{h} - \frac{2\lambda\sigma}{h^2+\lambda^2}\right] - \frac{m g_\odot}{(1+h/R_\odot)^2}, \tag{7}$$

where J is the total electric current inside the flux rope in units of I_0. The equilibrium in the system is realized as $F = 0$. This leads to (after normalization)

$$J\left(\frac{J}{h} - \frac{2\lambda\sigma}{h^2+\lambda^2}\right) = \frac{4.6032\times10^{-3}}{(1+5h/69.6)^2}, \tag{8}$$

compared to its counterpart appearing in Equations (2.10) and (2.11) of Forbes and Priest (1995). Another equation that governs both quasi-static and dynamic evolutions in the system is the frozen-flux condition on the surface of the flux rope, which reads as

$$J\ \ln\left(\frac{2h}{r_0}\right) + \sigma\ \tan^{-1}\left(\frac{\lambda}{h}\right) = J_m\ \ln\left(\frac{2J_m}{r_{00}}\right) + \sigma\ \tan^{-1}\left(\sqrt{\frac{2-T}{2+T}}\right), \tag{9}$$

where r_0 is the radius of the flux rope and is related to J and r_{00} such that $r_0 = r_{00}/J$. This relation of r_0 to J is an approximation of the solution for the force-free field inside the flux rope due to Parker (1974). Discussions about this approximation can be found in Isenberg, Forbes, and Démoulin (1993) and Lin, Forbes, and Isenberg (2001). Other notations appearing in Equation (9) are as follows:

$$\begin{aligned} T &= \frac{4.6032\times10^{-3}(1-5h/69.6)}{h(1+5h/69.6)^3}, \\ J_m &= \frac{\sigma}{4}\sqrt{4-T^2} + \sqrt{\frac{\sigma^2(4-T^2)}{16} + \frac{4.6032\times10^{-3}}{(1+5h/69.6)^2}}, \end{aligned} \tag{10}$$

where each notation is dimensionless. Obviously, only in the cases of weak magnetic field (small σ), does the impact of gravity on the system's evolution become important. For a given σ, the system evolves, under the control of Equations (8) and (9), in response to the change in λ, and eruption is triggered as λ decreases below a critical value, λ_c (see Forbes and Priest, 1996, for more discussions). Our calculations show that λ_c, together with the corresponding value of the flux rope height h_c, varies with σ in a weak manner. The variation in the background field is slow compared with that in the coronal magnetic field during the eruptions, so, the value of λ is fixed at λ_c in our consequent calculations for the evolution of the system following the catastrophe.

The fourth modification is related to the velocity of the flux rope in the eruptive process prior to the formation of the current sheet. This stage of the evolution starts with the catastrophe and ends with the flux rope reaching the height h^* at which an X-type neutral point appears on the boundary surface $y = 0$ and the current sheet begins to develop. The consequent evolution in the configuration including a current sheet is governed by equations in (1) with the following initial conditions:

$$t = t^*, \qquad h = h^*, \qquad \dot{h} = \dot{h}^*, \qquad p = 0, \qquad q = 0, \tag{11}$$

where we set $t = 0$ at the time the catastrophe starts thrusting the flux rope upwards, and t^* is the time when $h = h^*$. The height h^* and the corresponding J^* are determined by (see also Lin and Forbes, 2000)

$$J^* = \frac{h^*\sigma}{2\lambda}, \tag{12}$$

and Equation (9) with $\lambda = \lambda_c$ as well as the relation of r_0 to J.

In the process when the flux rope jumps from $h = h_c$ to $h = h^*$ (see Figure 1 of Lin and Forbes, 2000), the stored magnetic energy is converted into kinetic and gravitational potential energies. Therefore, the velocity of the flux rope is

$$\dot{h} = \sqrt{[W(h_c) - W(h)] + \frac{2.74 \times 10^{-2}(h_c - h)}{(1 + 5h_c/69.6)(1 + 5h/69.6)}}, \tag{13}$$

where

$$W(h) = \frac{25J^2}{4.2}\left[\ln\left(\frac{2hJ}{r_{00}}\right) + \frac{1}{2}\right],$$

J is calculated from (9) for given h, all the lengths are dimensionless and $\dot{h}$ is in units of $\dot{h}_0$. Because h_c is less than h as the eruption occurs, the velocity $\dot{h}$ given in Equation (13) is always smaller than its counterpart given in Equation (44) of Lin and Forbes (2000) for the case in which gravity was neglected. Furthermore, we pointed out that $W(h_c)$ is the total free energy that a magnetic configuration can store prior to the eruption (see the discussions of Isenberg, Forbes, and Démoulin, 1993; and Forbes, Priest, and Isenberg, 1994), and it is roughly quadratically related to J_c, the total current inside the flux rope as the system's evolution

approaches the critical point at which a transition from quasi-static evolution to dynamic evolution occurs. Investigating Equations (8), (9), and (10) indicates that J_c is approximately proportional to σ. Therefore, $W(h_c)$ is roughly proportional to σ^2, and the stronger the background field is, the more free energy can be stored prior to the eruption.

Combining Equations (9) and (10) with (13), one could determine J and $\dot{h}$ for a given h, and further calculate the corresponding time t when the flux rope reaches the height h. Then, the time t^* in (11) can thus be obtained. Lin (2002) indicates that h^* and t^* are linearly dependent on σ and $1/\sigma$, respectively. In the present case, on the other hand, the relations are no longer exactly linear due to the gravity, but h^* and t^* still increases and decreases monotonically with σ, respectively. This implies that the stronger the background field is, the earlier the current sheet forms, and the earlier the reconnection occurs. So, the time lag between the onset of CMEs and the associated flares depends on the strength of the background field. With all the parameters in (11) having been known, we are capable of solving the equations in (1) to get the variations of flux rope heights h, velocity $\dot{h}$, current sheet parameters p and q, etc., versus time t after the current sheet starts to form in the configuration. Combining the results at this stage with those within $0 \leq t \leq t^*$ yields the descriptions for the whole eruptive process.

3. Correlations between CMEs and Flares: Theories and Observations

As magnetic reconnection occurs in the current sheet, the associated flare is almost instantly initiated. The reconnection rate, which is prescribed by M_{A}, is in principle a function of time and parameters of the current sheet. Determination of this function self-consistently requires a time-dependent theory of strongly driven reconnection, but such a theory does not exist at the present time. However, it is known that in the coronal environment, M_{A} lies in the range between zero and unity (refer to Lin and Forbes, 2000; Forbes and Lin, 2000; and Webb *et al.*, 2003, for discussions in more detail). For simplicity, we take $M_{\mathrm{A}} = 0.1$ for our calculations in the present work.

The purpose of this part of the work is to investigate how the time of flare at maximum varies with the speed of the associated CME. Here, the time of flare at the maximum is identified with that of the output power P of the eruptive process, which is calculated from

$$P = F \cdot \dot{h} \tag{14}$$

for the stage of $0 \leq t \leq t^*$ with F and $\dot{h}$ given by (7) and (13), respectively, and from

$$P = m\dot{h}\frac{\mathrm{d}\dot{h}}{\mathrm{d}t} = m\dot{h}^2\dot{h}' \tag{15}$$

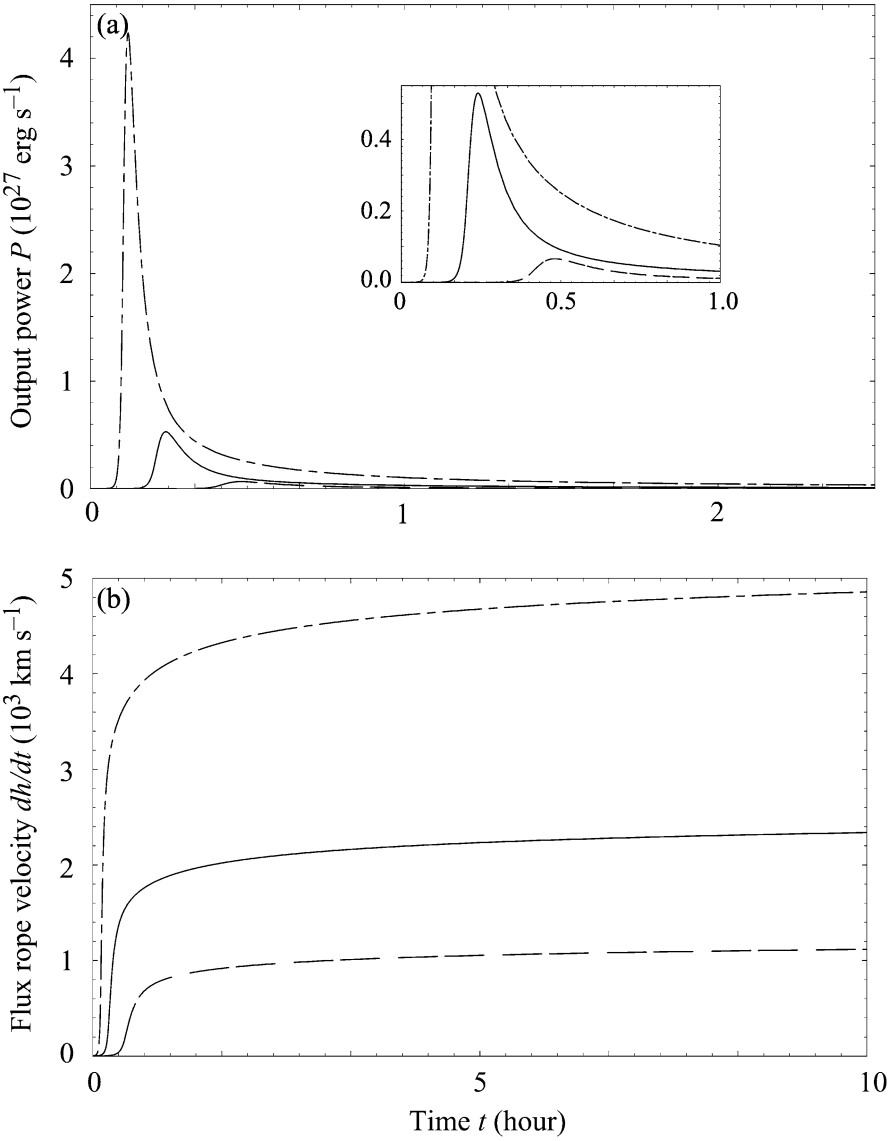

Figure 3. Variations of output power P (a) and CME velocity h (b) versus time t for $M_A = 0.1$ and various background fields: *dashed curves* for $\sigma = 0.5$, *solid curves* for $\sigma = 1.0$, and *dotted-and-dashed curves* for $\sigma = 2.0$. Same units are used for the inset.

for the stage of $t \geq t^*$ with $\dot{h}$ and $\mathrm{d}\dot{h}/\mathrm{d}t$ determined via solving equations in (1) with initial conditions in (11). As an example, Figure 3 plots variations in P and $\dot{h}$ versus time t for different background field σ, and shows that P reaches its maximum soon after reconnection commences.

Like Lin and Forbes (2000), we treat the flux rope as a projectile, the total released magnetic energy in the present case is partitioned into gravitational po-

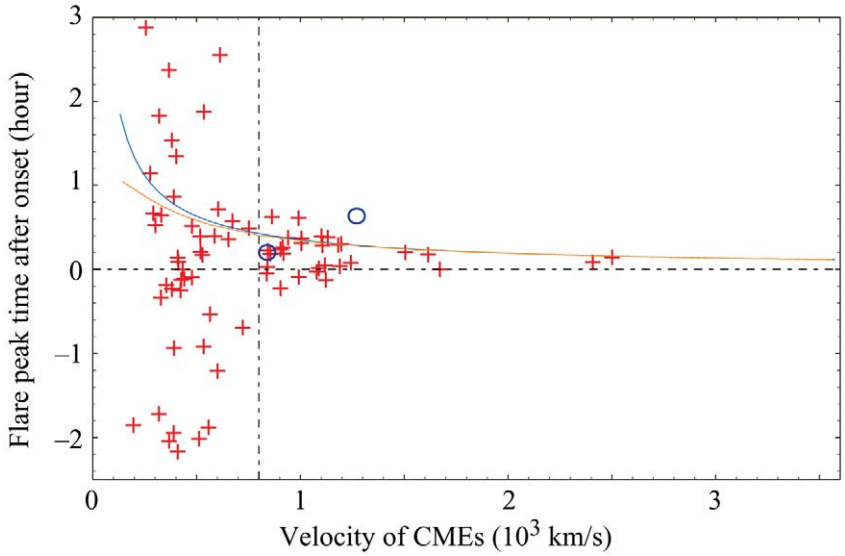

Figure 4. Variations of the time of flare at maximum versus the velocity of the associated CME. The horizontal axis starts at the onset of the eruption. *Red crosses* denote the observational results of Zhang *et al*. (2002) and *blue circles* denote those of Zhou, Wang, and Cao (2003). The *blue* and *yellow smooth curves* plot the theoretical results. The *blue curve* is for the case without including gravity, and the *yellow one* for that including the gravity. The *vertical dashed line* is used to separate the data for fast CMEs (*to the right*) from those for slow CMEs (*to the left*), and Zhang *et al*. (2002) artificially set it at 800 km s^{-1}. The *horizontal dashed line* is set at time zero.

tential and kinetic energy of the flux rope. Equations (2) and (7) indicate that the output power P defined by (14) and (15) accounts for the difference between the total energy released and the gravitational potential, namely P is due to the kinetic energy of the flux rope only. Lin and Forbes (2000) and Lin (2002) have pointed out that in reality much (perhaps as much as half) of the energy for P would go to heating and the wave energy associated with the generation of a fast-mode shock in front of the flux rope (CME).

For the time being, it is not quite clear in either theories or observations how fast the solar atmosphere could respond to the energy release during the eruption, and how the released magnetic energy partitions into kinetic energy of CMEs and thermal energy of flares. So, as an approximation, we assume that the time of P at maximum is identified with that of the associated flare at maximum, and that a half of P is used for thermal energy which is eventually consumed by the radiations of the flare in a wide band of wavelength. The partition of energy will decrease the velocities of CMEs calculated from either (2) or (13) by a factor of around $\sqrt{2}$.

Corresponding to the CME velocity, we can also determine the time of P at maximum for given σ. The variations in this time against the CME speeds are plotted by two continuous curves in Figure 4, the blue curve is for the case of neglecting gravity and the yellow one is for that including gravity. It is clear that

these two curves do not differ from one another for large velocities (also large σ), and the difference becomes apparent only as the velocity is less than 800 km s^{-1} which is indicated by the vertical dashed line (it will be discussed soon). The yellow curve indicates that gravity modestly decreases the velocities of CMEs, and this modification is not very significant unless the background field is so weak ($\sigma < 0.3$) that the free energy stored in the magnetic configuration is approaching the gravitational potential of the mass inside the flux rope. Here, we need to point out that although the time of P at maximum is plotted as a function of the speed of the associated CME, both of them are actually the functions of σ and are determined by σ monotonically. This fact will be useful for our discussions conducted in the sections afterward.

To compare the above results deduced from our theoretical calculations with those obtained from observations, we plot some related observational results in Figure 4 as well. The red crosses and blue circles in Figure 4 are taken from Zhang *et al*. (2002) and Zhou, Wang, and Cao (2003), respectively. The dashed vertical line is used by Zhang *et al*. (2002) to separate fast (toward the right) and slow (toward the left) CMEs. Although no clear boundary exists between slow and fast CMEs, a rough and artificial classification like this is still helpful. The dashed horizontal line is located at the time delay of zero. If the flare peaks after CME take off, the time delay is positive, otherwise negative. Their results show that most fast CMEs take off before the associated flares reach the maxima, and the flares associated with fast CMEs peak within a narrow time interval, while those associated with slow CMEs tend to occur at any time, so, the times of flares at maxima associated with slow CMEs spread in a wide range. This may be caused by the difficulties in precisely locating and timing the correct surface activities that are associated with slow CMEs, and in most cases there is just not an obvious surface event corresponding to a slow CME (Gopalswamy and Hanoaka, 1998; Zhang *et al*., 2003; Zhou, Wang, and Cao, 2003). So, the uncertainty of the data in this region should be fairly large, and it does not make much sense to compare the theory with observations in this region, but it is still qualitatively meaningful to notice the poor correlation of slow CMEs to solar flares.

Relative positions of our theoretical curves to the observational results (red crosses and blue circles) in Figure 4 suggest that the theories with respect to the CME model of Lin and Forbes (2000) reproduce the basic result of Zhang *et al*. (2002) regarding the CME–flare association. The consistency of our results with the observational data is particularly good for the fast CMEs that take off before the initiation of the associated flares.

However, we also noticed from Figure 4 that our results do not fit those eruptions during which the flares begin earlier than the associated CMEs. The discrepancy suggests that the eruptions with a flare appearing must first occur in magnetic configurations different from that investigated by Forbes and Priest (1995) and Lin and Forbes (2000). This is due to the fact that the behavior of correlation between CMEs and flares in an eruptive process depends as well on the relevant magnetic

environment or the magnetic structures. In the present work, as we have pointed out shortly, the magnetic configuration determines that the catastrophic loss of equilibrium starts before any magnetic reconnection site appears, so, the onset of a CME taking place in such kind of configuration always precedes the associated flare.

On the other hand, the similar catastrophic loss of equilibrium can also take place in other kinds of magnetic configurations, such as those investigated by Forbes and Isenberg (1991), Lin, Forbes, and Isenberg (2001), Lin and van Ballegooijen (2002), Isenberg, Forbes, and Isenberg (1993), Priest, Parnell, and Martin (1994) and Low (1990, as well as the references therein). In these magnetic environments, the site of magnetic reconnection, such as an X-type neutral point or a current sheet, may form before the catastrophe occurs (Figures (5a) and (5b)). In the cases discussed by Low (1990), Forbes and Isenberg (1991), Priest, Parnell, and Martin (1994), Amari *et al*. (2000), and Lin and van Ballegooijen (2002), no neutral point or current sheet exists at the very beginning. With the motion of the photospheric mass, the footpoints of these configurations in the regions of opposite magnetic polarities are brought towards one another. As two opposite-polarity magnetic fragments collide, a neutral point or a current sheet consequently forms between them. In the cases discussed by Lin, Forbes, and Isenberg (2001), the X-type neutral point or the current sheet may also be produced due to the newly emerging flux, and more than one neutral point could occur in the configuration prior to the eruption (Figure 5(c)).

When a new active region (with new magnetic flux) emerges on the photosphere, it interacts with those old or pre-existing structures via a layer. This layer could be a magnetic separatrix connecting to the neutral point or the current sheet, or it could be a quasi-separatrix layer (Démoulin *et al*., 1997), or it might just be an interface that separates two magnetic systems of different topological connections as shown in Figure 5(d) (Wang, 1998; Lin and Wang, 2002). Which structure eventually develops catastrophe depends on the relative polarities of the old and the new magnetic fragments as well as on the adjacent plasma conditions (Lin and Wang, 2002). Both analytic models (Lin, Forbes, and Isenberg 2001) and numerical simulations (Song, Wu, and Zhang, 1996; Podgorny and Podgorny, 2001) show that one (or more) X-type neutral point or a current sheet can develop as a new magnetic region appears in the vicinity of an old magnetic region.

Pre-existing magnetic reconnection sites makes it much easier for the fast reconnection and thus flares to commence at any time in the evolutionary process. Namely, the fast reconnection and significant heating may start either before, or after, or at the same time the catastrophe occurs. The consequent evolution of the system following the catastrophe is similar to what we have discussed in the present work. But the temporal sequences of the flare maximum and the onset of the CME may alternate accordingly. Within the framework of the sheared arcade model (Mikić and Linker, 1994) and the breakout model (Antiochos, DeVore, and Klimchuk, 1999) of CMEs, magnetic reconnection even works as a trigger of the

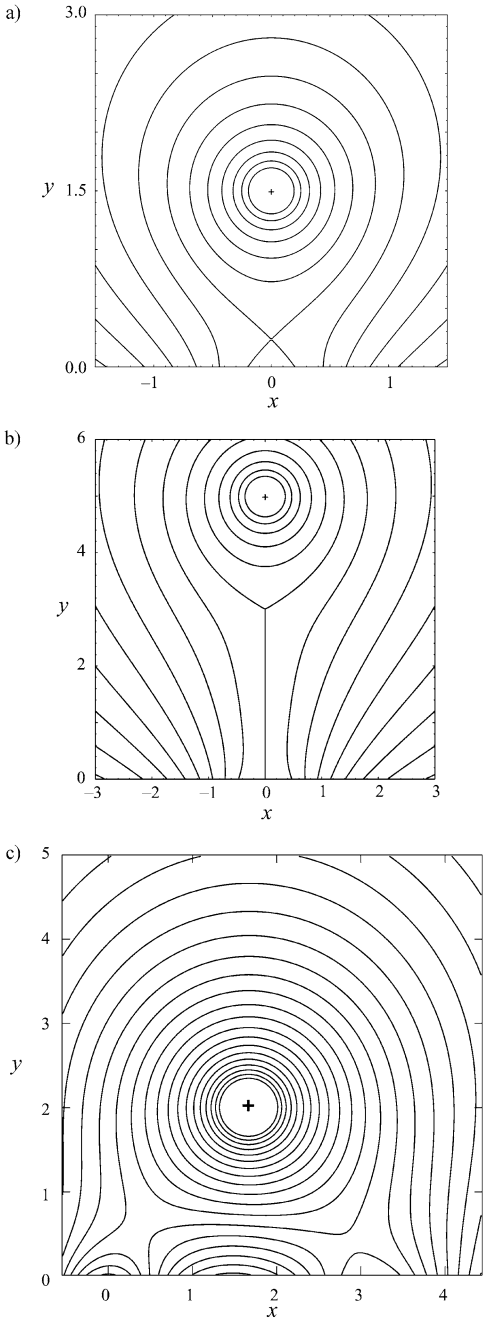

Figure 5. Magnetic configurations prior to the eruption, which include (a) a single X-type neutral point, (b) a vertical current sheet attached to the boundary surface, (c) two X-type neutral points, and (d) one X-type neutral point and one magnetic interface, and different colors are used to distinguish the magnetic field lines of different topological connections. The *cross* indicates the center of the flux rope.

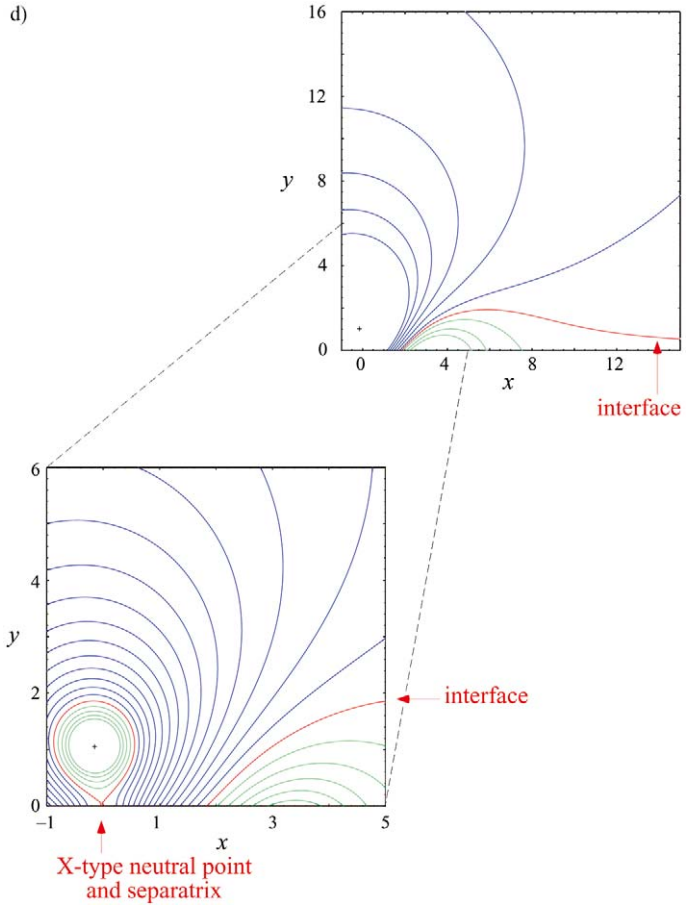

Figure 5. Continued.

eruption. So, in all of these cases, flares and other characteristics, such as rapid rise of soft X-ray emissions (Gallagher, Lawrence, and Dennis, 2003), which are tightly related to magnetic reconnection, should be manifested first by the eruption. This is fairly suggestive of the negative time lag of the flare as shown in Figure 4.

Before this section is ended, it is necessary to point out that the present work, together with those by Lin and Forbes (2000), Forbes and Lin (2000), and Lin (2002), is not able to treat the heating or flare process rigorously. Therefore, the way we determine the time of flare at maximum and the energy partitions in the present work cannot be considered rigorous and accurate in any sense. In reality, the parameters that describe these two important properties of an eruptive process depend in a significant way on both energy release and the local plasma and magnetic environment (compare the results of Forbes and Malherbe (1991) with those of Yokoyama and Shibata (1998)). The same energy release process may not necessarily cause the same flare manifestation. Recently, several numerical simulations

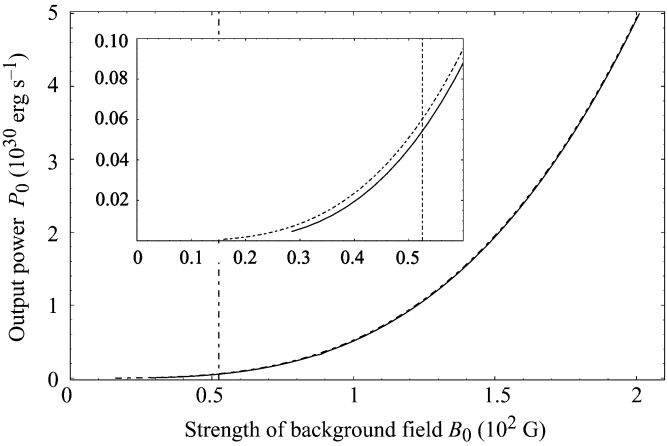

Figure 6. Variations of the output power of the eruption at maximum, P_0, versus the strength of the background field B_0. The *vertical dashed line* denotes the value of B_0 corresponding to the velocity of 800 km s^{-1} indicated by the vertical dashed line in Figure 2, it distinguishes the values of B_0 and P_0 for fast CMEs (*to the right*) from those for slow CMEs (*to the left*). Same units are used for the inset.

regarding CME processes and the relevant heating features have been conducted (Amari *et al.*, 2003; Linker *et al.*, 2003; Roussev *et al.*, 2003). Further investigations based on these works should be able to provide a more precise approach to flare timings and energy partitions of an eruptive process.

4. Energetics of Eruptive Processes and Strength of Background Field

As we have realized shortly that the free energy stored in a stressed magnetic structure prior to the eruption depends on the strength of the background field, the stronger the background field is, the more free energy can be stored, and thus the more energetic the eruptive process is. Here, the eruptive process refers to any disruption of the coronal magnetic field that causes either a flare, or eruptive prominence, or CME, or all of them. Lin (2002) discussed this issue and the CME-associations qualitatively. In this part of work, we are going to investigate what the above conclusion means to the CME–flare associations quantitatively. We believe that a comprehensive understanding of the energetics of an eruptive process is essential for us to learn the physical nature of the observed eruptions. The correlations among different manifestations such as solar flares, eruptive prominences and subsequent eruptive CMEs will be important if two or all of them can be observed in a single eruptive process.

On the basis of the calculations made in last section, we are then able to obtain the value of P at maximum, P_0, and plot P_0 against the background field σ (Figure 6), where P_0 is in units of 10^{30} erg s^{-1}. The dashed curve is for the case without including gravity, and the solid one is for that including gravity. The two

curves are almost identical with one another for a strong background field ($\sigma > 0.5$ with difference $< 10\%$). The difference becomes large as σ is too small, and it exceeds a factor of 1.5 (e.g., the difference between 4.62×10^{-3} and 7.03×10^{-3}) as $\sigma < 0.3$. Because of the scale we are using for Figure 6, this difference is not very obvious even for small σ. The vertical dashed line corresponds to that in Figure 4, separating the values of σ for fast CMEs (toward the right) and those for slow CMEs (toward the left).

As we have noted, there could be as much as half of the released magnetic energy related to P going to heating plasma and the wave energy associated with the generation of a fast-mode shock in front of the CME. Suppose this part of energy goes equally to the heating and to the wave energy, then heating consumes a quarter of the released energy associated with P. Therefore, a fraction of 25% of P_0 obtained in our calculation should be responsible for the radiation from the flare at maximum during an eruptive process, and we are thus able to estimate the lower limit of P_0 as well as the corresponding σ required for an eruptive process during which both flare and CME can be observed. This could be done by analyzing the existing results for a specific event.

Canfield *et al*. (1980) conducted a unique study: for the first time, they had measured the radiative energy output of a single flare over a range of more than decades in wavelength from below 1 Å to above a meter. Webb *et al*. (1980) investigated the macroscopic mass motions, including a surge and an eruptive prominence (or CME), in the same event. The flare was observed on 5 September 1973, it is not a major one, but a class 1N flare. The X-ray and XUV emission was mainly from the plasma in a group of simple looplike structures (Dere, Horan, and Kreplin, 1977). Its relative simple structure and large size makes it possible for a rather detailed analysis.

Before Canfield *et al*. (1980) and Webb *et al*. (1980), this flare and its pre-flare manifestations had been studied by many authors (Cheng and Widing, 1975; Brueckner, 1976; Vorphal, 1976; Kahler, Krieger, and Vaiana, 1975; Dere, Horan, and Kreplin, 1977; and Van Hoven *et al.*; 1980). It was chosen for analysis because it was well observed from both *Skylab* and Earth. Using the data they were able to collect, Canfield *et al*. (1980) brought the total radiative power output at the maximum of the flare to around 10^{27} erg s^{-1}, as well as the total energy radiated by the flare around 4×10^{29} ergs. Meanwhile, the results of Webb *et al*. (1980) indicated that the associated eruptive prominence (or CME) is slow with involved mass in the range 8.3×10^{13}–5.0×10^{14} g and velocity of 465 km s^{-1}, and that the mass of the surge varies from 3×10^{15}–3×10^{16} g and the velocity is 200 km s^{-1}. They further obtained the estimations for the kinetic energy (K.E.), change in the gravitational potential energy (P.E.), and the total mechanical energy (M.E.) of both the associated CME and the surge, which are listed in Table I. Based on these data and Figures B.6 and B.8 of Webb *et al*. (1980), we are able to estimate the related powers output and their maxima. We found that for the eruptive prominence, the maximum of power output related to its kinetic energy varies from

TABLE I

Data taken and deduced from the work of Webb *et al*. (1980).

Objective	Mass[a]	K. E.[b]	P. E.[b]	M. E.[b]	P_0[c]
CME	0.83 - 5.0	0.16 - 3.2	0.12 - 0.82	0.27 - 3.8	0.20 - 1.20
Surge	30 - 300	0.26 - 6.6	5.1 - 79	5.3 - 85	1.23 - 1.91

[a]in units of 10^{14} g.
[b]in units of 10^{29} erg.
[c]in units of 10^{27} erg s^{-1}.

1.98×10^{26} erg s^{-1} to 1.02×10^{27} erg s^{-1}, and for the surge, it is in the range 1.23×10^{27}–1.91×10^{27} erg s^{-1}, which are also listed in Table I (see column 6).

From the plots for kinetic and total mechanical energies in Figure B.6 and B.8 of Webb *et al*. (1980) as well as the results of Canfield *et al*. (1980), we further notice that the time of the flare at maximum, and those of kinetic energy and mechanical energy of both CME and surge at maxima do not differ from one another very significantly. Our estimation indicates that the difference is less than 7 min. As an approximation, we consider them to occur simultaneously. Therefore, the upper limit of the total power output for the flare radiation and macroscopic mass motions at maximum during the eruption on September 5, 1973 is about 3.93×10^{27} erg s^{-1}. Considering the fact that this flare is not a major one, we could take $P_0 = 3.93 \times 10^{27}$ erg s^{-1} as the lower limit of the power output of an eruptive process at maximum, which manifests flare, mass ejection, as well as the associated consequences in the outermost corona and interplanetary space.

If we draw a horizontal line at $P_0 = 3.93 \times 10^{27}$ erg s^{-1} in Figure 6, we would get two intersections of this line at $\sigma = 0.28$ and at $\sigma = 0.24$ with solid and dashed curves, respectively. According to the calculations based on the formulae given in previous sections, these two values of σ lead to CME speeds of 80 km s^{-1} if gravity is considered, and 247 km s^{-1} if gravity is neglected. The difference is obviously due to gravity. Furthermore, our calculations also indicate that the solid curve in Figure 6 and the yellow curve in Figure 4 do not extend to $\sigma = 0$, instead both of them terminate at around $\sigma = \sigma_c = 0.27$. This implies that the effect of gravity on the eruption becomes significant enough to prevent the CME from propagating if the magnetic field in the related configuration is too weak, say weaker than 27 G which is a kind of critical strength of the background field related to the CME propagation.

Isenberg, Forbes, and Démoulin (1993) found that the effect of gravity near the solar surface on the evolution of a magnetic system that includes a flux rope with mass of 10^{16} g is equivalent to that of a magnetic field of 17 G, and the catastrophic loss of equilibrium in the system can be prevented if the strength of the background field is lower than this value, instead the system will evolve smoothly in response to the slow change in the boundary conditions. Accordingly, the evolution in the

corresponding system is quite likely to end up with a slow CME in the way similar to what Lin and van Ballegooijen (2002) have discussed. Forbes (2003, private communication) also points out that the gravity of the filament or prominence may play an important role in the process of slow CMEs by prohibiting the catastrophe to occur at the very beginning. The background field utilized by Isenberg, Forbes, and Démoulin (1993) is produced by a quadrupole beneath the photosphere, and that in the present work is produced by two point-source regions on the boundary surface. This may cause the difference between the critical strengths in two cases, but the difference should not be so large as directly indicated by the numbers since the mass used in the present work is more than two times that used by Isenberg, Forbes, and Démoulin (1993).

The masses of CMEs inferred from *SOLWIND* observations from 1979 to 1981 (Howard *et al.*, 1985) ranged from 2×10^{14} to 4×10^{16} g, with an average value of 4.1×10^{15} g. This range of values of CME masses does not change over the decades. Until recently, the largest measured values of CMEs with eruptive prominences that have been observed are still a few times 10^{16} g (Howard *et al.*, 1997; and D. F. Webb, 2003, private communications), and the lowest measured value is still a few times 10^{14} g (Ciaravella *et al.*, 2001). So, the total mass in the flux rope, 2.1×10^{16} g, applied to the calculations in the present work, is almost the upper limit of the CME masses, and for the CME with the average mass, the value of σ_c should be lower than 0.27 G.

Obviously, the value of σ_c should also vary with the specific background fields applied. The existence of σ_c indicates that the free energy stored in a stressed magnetic configuration with background field weaker than σ_c is not enough to account for both flare and CME in a single eruptive process, instead it may just be able either to drive the closed magnetic field outward smoothly producing a slow CME without significant heating (refer to Lin and van Ballegooijen, 2002, for an alternative explanation of slow CMEs), or to heat the plasma within the closed magnetic structures without stretching the whole structure outward. This apparently explains why slow CMEs are poorly associated with solar flares, and why there are generally no large-scale mass and magnetic flux ejections observed during the processes of small flares (refer to Švestka, 1976; Priest, 1982), either.

Combining the first conclusion with the information revealed by Figures 4 and 6 indicates that slow CMEs generally occur in the regions of weak magnetic field and fast CMEs are more likely to be observed in the regions of strong magnetic field, and that the difference in energetics between weak field and strong field yields the difference in the correlations of solar flares with slow CMEs and with fast CMEs. These consequences, in fact, confirm the statement of Švestka (2001; 2002, private communication) that there is no difference in principle between slow and fast CMEs, and that the occurrence and absence of flares in relation to CMEs depends exclusively on the strength of the magnetic field in which the eruption is initiated. Because the CME–flare association depends on the free energy stored in the magnetic configuration prior to the eruption, the above consequences also

indirectly prove the speculation made by St. Cyr and Webb (1991) a decade ago that 'the slow mass ejections are poorly associated simply because any Hα, X-ray, and radio signature accompanying the ejections are weak and tie below the sensitivity threshold of instruments presently used in synoptic solar observation'.

5. Comparison between the Two Correlations

After having comprehensively worked out the physics behind the correlation between CMEs and solar flares, it is also worth investigating the correlation between CMEs and eruptive prominences. These two correlations are generally believed to be equally important for understanding the physical nature of eruptive processes, and they are usually discussed with the same weight (Moon *et al.*, 2002; Zhou, Wang, and Cao, 2003, and references therein). In fact, however, the details of the physical processes of solar flares and eruptive prominences are basically different although both of them result from magnetic energy release occurring in the corona. The solar flare is the reaction of the solar atmosphere to the fast magnetic dissipation, or magnetic reconnection, occurring in the corona. It is a secondary effect of the magnetic energy release. No reconnection, no flare. However, the reconnection is not the necessity for the eruptive prominence that can directly result from the instabilities or the loss of equilibria in the relevant magnetic structures (cf., Forbes and Isenberg, 1991; Isenberg, Forbes, and Démoulin, 1993; Lin and Forbes, 2000; Low, 2001). In principle, disruption occurring in a magnetic structure results from the interaction between the current and the magnetic field in the relevant configuration. As indicated by both observations (e.g., Hundhausen, 1999) and theoretical calculations (e.g., Mikić and Linker, 1994; Antiochos, DeVore, and Klimchuk, 1999; Lin and Forbes, 2000; Lin, 2002), a coronal mass ejection process thrusts not only the plasma but also the stressed (or twisted) magnetic structure into the outermost corona and interplanetary space. It is this stressed structure, which is associated with the electric current concentration, that contains the mass prior to the eruption and brings the mass away from the Sun during the eruption.

According to the typical values of the properties of a quiescent prominence given by Tandberg-Hanssen (1974), Jensen, Maltby, and Orrall (1979), and also Priest (1982), we obtain the typical value of the mass contained by a prominence, 4.52×10^{15} g, which is about the average value of the mass involved in the CME process. The typical masses of quiescent and active prominences do not differ from one another too much although other parameters, such as temperature and magnetic field, do (e.g., Tandberg-Hanssen, 1974; Jensen, Maltby, and Orrall, 1979; Priest, 1982). So, whether a CME goes with a prominence eruption depends on whether the relevant structure prior to the eruption contains enough plasma, and also on how well the mass concentration and the electric current concentration coincide with one another in space. In other words, if a magnetic configuration prior to the eruption includes enough mass and the mass concentration coincides with the

current concentration in space, then the CME developing from this configuration must start with an eruptive prominence, otherwise, the CME may occur without an apparent associated prominence eruption.

Over the decades, every broad study of the occurrence of solar activities on the disk near the times and locations of observed CMEs (Munro *et al*., 1979; Webb and Hundhausen, 1987; St. Cyr and Web, 1991; St. Cyr *et al*., 1199; Moon *et al*., 2002; Zhou, Wang, and Cao, 2003) has found the most common form of associated activity to be the eruption of a prominence. However, there are still many CMEs that are observed without a prominence eruption associated, and with no hint of an interior feature in the mass ejection itself (see also Hundhausen, 1999). Harrison (1986) gives three examples of such events, which were observed by SMM and other ground-based instruments and have been well studied by various authors on different aspects (Poland *et al*., 1982; Antonucci *et al*., 1982; Stewart *et al*., 1982; Wu *et al.*, 1983; Gary *et al.*, 1984; Harrison, 1985).

The first event manifested a slow CME at speed of around 250 km s^{-1} and an X-ray flare of class M4 (Antonucci *et al*., 1982; Poland *et al*., 1982; Wu *et al*., 1983). A fairly large amount of the magnetic energy released during this event seems to go to the thermal energy of the flare since extremely high temperature emissions from ions Fe XXI, Fe XXV, Ca XIX and S XV were observed. (These four spectral lines have peak formation temperatures of 1.1×10^7, 1.87×10^7, 3.5×10^7, and 1.6×10^7 K, respectively.) The material in the ejecta was mainly observed in O V (2.5×10^5 K) and Fe XXI (Poland *et al*., 1982), the total electron density of this part of material varies from 2.75×10^{10} to 4.84×10^{10} cm^{-3}, and the estimated volume is in the range 3.9×10^{26}–2.7×10^{27} cm^3 (Wu *et al*., 1983). Assuming a 2% helium composition, we deduce an estimation of the total mass ejected during this event ranging from 2.15×10^{13} to 2.42×10^{14} g. This might just be a lower limit since there may be other spectral components in the ejecta that were not observed.

The second event was a CME with speed of ~ 700 km s^{-1} associated with an M3 flare and Types III and II/V radio bursts (Gary *et al*., 1984). It had an onset coincident in time with a weak, pre-flare, soft X-ray burst (Harrison *et al*., 1985). Based on the information revealed from their radio observations, Gary *et al*. (1984) brought the total mass ejected in this event to $\sim 7.5 \times 10^{14}$ g. The third event started with a flare-spray in Hα, Type III and X-ray bursts. The CME was associated with a C6 flare, its leading edge propagated at velocity $\sim$ 750 km s^{-1} and rear edge at $\sim$ 560 km s^{-1}, which implies an expansion at velocity of 190 km^{-1} (Stewart *et al*., 1982). The analysis of Stewart *et al*. brought the total ejected mass to 10^{14}–10^{15} g.

We noticed that the above three examples include both slow and fast CMEs, but none of them had an associated filament eruption, and the total masses ejected in the processes are all less than the typical value of prominence masses, 4.52×10^{15} g, and the average value of CME masses, 4×10^{15} g. This seems to suggest that the poor correlation between CMEs and eruptive prominences may be due to the small amount of plasma contained in the disrupted magnetic structure, and that the

typical value of prominence mass is the criterion for the CME–eruptive prominence association.

This may not be a quantitatively rigorous conclusion because the lower time and spatial resolutions of the early observations could limit our capabilities of recognizing small and fast features on the surface when the eruption occurred. A low-mass CME observed recently by three instruments, EIT, LASCO and UVCS, on board the SOHO satellite is quite likely to be associated with a small prominence eruption. The data analysis for this event indicates that the total mass ejected is a few times 10^{14} g (Ciaravella *et al.*, 2000). But the amount of mass and the mass concentration should be important for the CME–eruptive prominence association. It is worth paying more attention to this aspect in the future.

6. Conclusions

On the basis of the widely accepted understanding that the driver behind solar flares, eruptive prominences and CMEs is the relaxation of highly stressed coronal magnetic fields which have been driven to a complex state by photospheric motions (Harrison, 1996), and of a specific model developed by Lin and Forbes (2000), we investigated the correlations of CMEs with solar flares and with eruptive prominences. The investigation of the CME-flare association is quantitative. With modified formulae of Lin and Forbes (2000) and Lin (2002), for the first time, the effects of gravity on CME propagation is incorporated in the catastrophic models of CMEs. Our results indicate that the strength of magnetic field and the magnetic structure in the configuration prior to the eruption determine the correlation between CMEs and flares, and that the importance of gravity becomes significant as the strength of magnetic field in this configuration is weak.

Our discussion of the CME–eruptive prominence association is qualitative, the results deduced from observations seem to suggest that this association depends on the amount and the concentration of the total mass in the relevant magnetic structure. The main results of the present work are summarized as follow:

(1) For a disruption of the coronal magnetic field, the stronger the background field is, the faster the CME is, and the more apparent the correlation between CME and flare is.

(2) The difference in the times of the CME onset and the associated flare at maximum depends on both the background field strength and the structure of the disrupted magnetic field. In the magnetic configuration such as those studied by Forbes and Priest (1995), the CME onset precedes the associated flare, and the time interval that the flare at maximum lags behind the onset of the associated CME decreases approximately linearly with the strength of the background field. In other magnetic configurations such as those studied by Low (1990), Forbes and Isenberg (1991), Priest *et al.* (1994), and Isenberg *et al.* (1993), the flare may appear first, but further quantitative investigations on the time lag are needed.

(3) The impact of gravity on the above correlation is not important until the background field in the disrupted magnetic structure is too weak, say weaker than 30 G. As expected, the role played by gravity is to reduce the CME velocity. With the field strength further decreasing, the free energy stored in the configuration may not be enough to drive both the flare and the CME in a single eruptive process. We are only able to expect either a flare or a CME to be observed, namely the resultant correlation between CME and flare is poor or even vanishes. In the present work, the magnetic field, whose strength at the photosphere is less than 27 G, is regarded as weak.

(4) In addition to the field strength and the structure in the disrupted magnetic field in the corona, the correlation between CME and eruptive prominence also depends on the total amount and the concentration of the plasma mass in the related magnetic configuration. Our qualitative discussion yields that with a mass concentration coincident with the current concentration in space and with the total amount of mass exceeding 4.52×10^{15} g, which is about the typical value of the prominence masses, the CME may commence with an apparent prominence eruption. Further quantitative investigation on this issue is worthwhile.

(5) These correlations are quite suggestive of that the flare, CME, and any eruptive prominence are constituents of the same active event (Harrison, 1996), and that these three eruptive phenomena are different manifestations in different hierarchies of the solar atmosphere at different evolutionary stages of a single process that involves energy release in a disruption of the coronal magnetic field. A recent work by Wang *et al*. (2003) can be considered as an endorsement of our conclusions.

(6) Finally, several important issues related to the model we used in the present work need to be mentioned. First, our work is based on a simple two-dimensional model, some realistic three-dimensional effects, such as anchoring the ends of the flux rope in the photosphere, remain unknown. Even though Webb *et al*. (2003) recently evaluate many positive aspects of this simple model from the point of views of observers, a comprehensive three-dimensional description of CME is still necessary. Second, a great deal of work is needed to determine the effects of shocks, reconnection heating, and the solar wind on the eruptive process. Hopefully, more realistic models including these effects will be developed in the near future.

Acknowledgements

The author appreciates M. Zhang for providing the raw data of observations. The author is also grateful to T. G. Forbes, A. A. van Ballegooijen, W. Soon, as well as the anonymous referees for helping improve the manuscript. This work is supported by NASA under the grants NAG5-12865 and NAG5-12827 of the Smithsonian Astrophysical Observatory.

References

Alexander, D., Metcalf, T. R., and Nitta, N. V.: 2002, *Geophys. Res. Lett.* **29** (10), 41–1.

Aly, J. J.: 1984, *Astrophys. J.* **683**, 349.

Aly, J. J.: 1991, *Astrophys. J.* **375**, L61.

Amari, T., Luciani, J. F., Mikić, Z., and Linker, J. A.: 2000, *Astrophys. J.* **529**, L49.

Amari, T., Luciani, J. F., Aly, J. J., Mikić, Z., and Linker, J. A.: 2003, *Astrophys. J.* **585**, 1073.

Andrews, M. D., and Howard, R. A.: 2001, *Space Sci. Rev.* **95**, 147.

Antiochos, S. K., DeVore, C. R., and Klimchuk, J. A.: 1999, *Astrophys. J.* **510**, 485.

Antonucci, E., Gabriel, A. H., Acton, L. W., Culhane, J. L., Doyle, J. G., Leibacher, J. W., Machado, M. E., Orwig, L. E., and Rapley, C. G.: 1982, *Solar Phys.* **78**, 107.

Brueckner, G. E.: 1976, *Phil. Trans. Roy. Soc. London* **A281**, 443.

Burkepile, J. T., Darnell, J. A., and DeToma, G.: 2002, AGU Fall Meeting, abstract SH61A-0431.

Canfield, R. C., Cheng, C.-C., Dere, K. P, Dulk, G. A., McLean, D. J., Robinson, R. D., Jr., Schmahl, E. J., and Schoolman, S. A.: 1980, in P. Sturrock (ed.), *Solar Flares*, Colorado Assoc. University Press, Boulder, pp. 451–469.

Cheng, C.-C., and Widing, K.: 1975, *Astrophys. J.* **201**, 735.

Dere, K. P., Horan, D. M., and Kreplin, R. W.: 1977, *Astrophys. J.* **217**, 976.

Dere, K. P., Brueckner, G. E., Howard, R. A., Michels, D. J, and Delaboudinière, J. P.: 1999, *Astrophys. J.* **516**, 645.

Dryer, M.: 1996, *Solar Phys.* **169**, 421.

Forbes, T. G.: 2003, *Proceedings of The 34th COSPAR Scientific Assembly*, in press.

Forbes, T. G. and Acton, L. W.: 1996, *Astrophys. J.* **459**, 330.

Forbes, T. G. and Isenberg, P. A.: 1991, *Astrophys. J.* **373**, 294.

Forbes, T. G. and Lin, J.: 2000, *J. Atmospheric Solar Terrest. Phys.* **62**, 1499.

Forbes, T. G. and Malherbe, J. M.: 1991, *Solar Phys.* **135**, 361.

Forbes, T. G. and Priest, E. R.: 1995, *Astrophys. J.* **446**, 377.

Forbes, T. G., Priest, E. R., and Isenberg, P. A.: 1994, *Solar Phys.* **150**, 245.

Gallagher, P., Lawrence, G., and Dennis, B.: 2003, *Bull. Am. Astron. Soc.* **35**, 511.

Gary, D. E., Dulk, G. A., House, L., Illing, R., Sawyer, C., Wagner, W. J., McLean, D. J., and Hilder, E.: 1984, *Astron. Astrophys.* **134**, 222.

Gosling, J. T., Hilder, E., MacQueen, R. M., Munro, R. H., Poland, A. I., and Ross, C. L.: 1976, *Solar Phys.* **48**, 389.

Guhathakurta, M., Holzer, T. E., and MacQueen, R. M., 1996, *Astrophys. J.* **458**, 817.

Harrison, R. A.: 1986, *Astron. Astrophys.* **162**, 283.

Harrison, R. A.: 1996, *Solar Phys.* **166**, 441.

Howard, R. A., Sheeley, Jr., N. R., Koomen, M. J., and Michels, D. J.: 1985, *J. Geophys. Res.* **90**, 1356.

Howard, R. A., Brueckner, G. E., St. Cyr, O. C. *et al.*: 1997, in N. Crooker, J. A. Joselyn, and J. Feynman (eds.), *Coronal Mass Ejections* AGU, Washington DC, pp. 15–26.

Hundhausen, A. J.: 1988, in V. Pizzo, T. E. Holzer, and D. G. Sime (eds.), *Proceedings of The Sixth International Solar Wind Conference*, NCAR, Boulder, pp. 181–214.

Hundhausen, A. J.: 1999, in K. T. Strong, J. L. R. Saba, B. M. Haish, and J. T. Schmelz (eds.), *The Many Faces of The Sun: A Summary of The Results from NASA's Solar Maximum Mission*, Springer-Verlag, New-York, pp. 143–200.

Isenberg, P. A., Forbes, T. G., and Démoulin, P.: 1993, *Astrophys. J.* **417**, 368.

Jensen, E., Maltby, P., and Orrall, F. Q. (eds.): 1979, 'Phys of Solar Prominences', *IAU Colloq.* **44**.

Kahler, S. W.: 1992, *Annu. Rev. Astron. Astrophys.* **30**, 113.

Kahler, S. W., Krieger, A. S., and Vaiana, G. S.: 1975, *Astrophys. J.* **199**, L57.

Kopp, R. A. and Pneuman, G. W.: *Solar Phys.* **50**, 85.

Leblanc, Y., Dulk, G. A, and Bougeret J.-L., 1998, *Solar Phys.* **183**, 165.

Lin, J.: 2001, 'Theoretical Mechanisms for Solar Eruptions', Ph.D. thesis, Physics Dept. University of N. H., Durham.
Lin, J.: 2002, *Chinese J. Astron. Astrophys.* **2**, 539.
Lin, J. and Forbes, T. G.: 2000, *J. Geophys. Res.* **105**, 2375.
Lin, J. and van Ballegooijen, A. A.: 2002, *Astrophys. J.* **576**, 485.
Lin, J. and Wang, J.: 2002, in H. Wang and R. Xu (eds.), *Proceedings of the COSPAR Colloq. on Solar-Terrest. Mag. Act. & Space Envir.*, Pergamon, Boston, pp. 137–143.
Lin, J., Forbes, T. G., and Isenberg, P. A.: 2001, *J. Geophys Res.* **106**, 25053.
Linker, J. A., Mikić, Z., Lionello, R., Riley, P., Amari, T., and Odstrcil, D.: 2003, *J. Plasma Phys.*, in press.
Low, B. C.: 1990, *Annu. Rev. Astron. Astrophys.* **28**, 491.
Low, B. C.: 2001, *J. Geophys. Res.* **106**, 25141.
Low, B. C and Zhang, M.: 2002, *Astrophys. J.* **564**, L53.
MacQueen, R. M. and Fisher, R. R.: 1983, *Solar Phys.* **89**, 89.
Mikić, Z. and Linker, J. A.: 1994, *Astrophys. J.* **430**, 898.
Moon, Y.-J., Choe, G. S., Wang, H., Park, Y. D., and Gopalswamy, N.: 2002, *Astrophys. J.* **581**, 694.
Neupert, W. M., Thompson, B. J., Gurman, J. B., Plunkett, S. P.: 2001, *J. Geophys. Res.* **106**, 25215.
Parker, E. N.: 1974, *Astrophys. J.* **191**, 245.
Phillips, J. L., Goldstein, B. E., Gosling J. T., HamFond, C. M., Hoeksema, J. T., and McComas, D. J., 1995, *Geophys. Res. Lett.* **22**, 3305.
Podgornyĭ, A. I., and Podgornyĭ, I. M.: 2001, *Astron. Rep.* **45**, 71.
Priest, E. R.: 1982, *Solar MHD*, D. Reidel Publ. Co., Dordrecht, Holland.
Priest, E. R., Parnell, C. E., and Martin, S. F: 1994, *Astrophys. J.* **427**, 459.
Roussev, I. I., Forbes, T. G., Gombosi, T. I., Sokolov, I. V., DeZeeuw, D. L., and Birn, J.: 2003, *Astrophys. J.* **588**, L45.
Sheeley Jr., N. R., Walters, J. H., Wang, Y.-M., and Howard, R. A.: 1999, *J. Geophys. Res.* **104**, 24739.
Sittler, E. C., Jr. and Guhathakurta, M.: 1999, *Astrophys. J.* **523**, 812.
Song, M. T., Wu, S. T., and Zhang, H. Q.: 1996, *Solar Phys.* **167**, 57.
Srivastave, N., Schwenn, R., Inhester, B., Stenborg, G., and Podlipnik, B.: 1999, in S. R. Habbal, R. Esser, J. V. Hollweg, and P. A. Isenberg (eds.), *Solar Wind Nine*, The American Institute of Physics/Woodbury, New York, pp. 115–118.
St. Cyr, O. C. and Webb, D. F.: 1991, *Solar Phys.* **136**, 379.
Stewart, R. T., Dulk, G. A., Sheridan, K. V., House, L., Wagner, W. J., Sawyer, C., Illing, R.: 1982, *Astron. Astrophys.* **116**, 217.
Sturrock, P. A.: 1991, *Astrophys. J.* **380**, 655.
Švestka, Z.: 1976, *Solar Flares*, D. Riedel Publ. Co., Dordrecht, Holland.
Švestka, Z.: 1986, in D. F. Neidig (ed.), *The Lower Atmosphere of Solar Flares*, NSO/SacPeak Publ., pp. 332–355.
Švestka, Z.: 1995, *Solar Phys.* **160**, 53.
Švestka, Z.: 2001, *Space Sci. Rev.* **95**, 135.
Švestka, Z. and Cliver E. W.: 1992, in Z. Švestka, B. V. Jackson, and M. E. Machado (eds.), *Eruptive Solar Flares*, Springer-Verlag, New York, pp. 1–14.
Tandberg-Hanssen, E.: 1974, *Solar Prominences*, D. Reidel Publ. Co., Dordrecht, Holland.
Van Hoven, G., Anzer, U., Barbosa, D. D., Birn, J., Cheng, C.-C., Hansen, R. T., Jackson, B. V., Martin, S. F., McIntosh, P. S., Nakagawa, Y., Priest, E. R., Reeves, E. M., Reichmann, E. J., Schmal, E. J., Smith, J. B., Solodyna, C. V., Thomas, R. J., Uchida, Y., and Walker, A. B. C.: 1980, in P. A. Sturrock (ed.), *Solar Flares*, Colorado Assoc. University Press, Boulder, pp. 17–81.
Van Tend, W.: 1979, *Solar Phys.* **61**, 89.
Van Tend, W. and Kuperus, M.: 1978, *Solar Phys.* **59**, 115.
Vorphal, J. A.: 1976, *Astrophys. J.* **205**, 868.

Wagner, W. J.: 1984, *Ann. Rev. Astron. Astrophys.* **22**, 267.
Wang, H., Qiu, J., Jing, J., and Zhang, H.: 2003, *Astrophys. J.* **593**, 564.
Webb, D.F., Cheng, C.-C., Dulk, G. A., Edberg, S. J., Martin, S. F., McKenna Lawlor, S., and McLean, D. J.: 1980, in P. A. Sturrock (ed.), *Solar Flares*, Colorado Assoc. University Press, Boulder, pp. 471–499.
Webb, D. F., Burkepile, J., Forbes, T. G., and Riley, P.: 2003 *JGR*, in press.
Riley, P.: 2003, *JGR*, in press.
Wu, S. T., Wang, S., Dryer, M., Poland, A. I., Sime, D. G., Wolfson, C. J., Orwig, L. E., and Maxwell, A.: 1983, *Solar Phys* **85**, 351.
Yokoyama, T. and Shibata, K.: 1998, *Astrophys. J.* **494**, L113.
Zhang, J., Dere, K. P., Howard, R. A., Kundu, M. R., and White, S. M.: 2001, *Astrophys. J.* **559**, 452.
Zhang, J., Dere, K. P., Howard, R. A., and Bothmer, V.: 2003, *Astrophys. J.* **582**, 520.
Zhang, M., Golub, L., DeLuca, E., and Burkepile, J.: 2002, *Astrophys. J.* **574**, L97.
Zhou, G., Wang, J., and Cao, Z.: 2003, *Astron. Astrophys.* **397**, 1057.